

## XIX-12. Determination of the Energy Band Parameters of Bismuth by Giant Quantum Attenuation of Sound Waves\*

Y. SAWADA and E. BURSTEIN

*Physics Department and Laboratory for Research on the Structure of Matter  
 University of Pennsylvania, U.S.A.*

and

L. TESTARDI

*Bell Telephone Laboratories, Incorporated, Murray Hill,  
 New Jersey, U.S.A.*

Giant quantum attenuation of sound waves was studied in bismuth for the Faraday configuration using 930 Mc longitudinal wave and magnetic field up to 100 kg. The observed attenuation peaks were "spike" shaped and exhibited well defined spin splittings. Cyclotron masses and spin masses for electrons and holes were determined from the attenuation peaks. The line shape of giant quantum attenuation peaks was studied for the non-parabolic energy band model. Non-linear acoustic attenuation and "transverse magneto-acousto-electric effect" were discussed.

### § 1. Introduction

Giant quantum attenuation (GQA) for longitudinal sound waves was first predicted by Gurevich *et al.*<sup>1)</sup> Later Quinn<sup>2)</sup> investigated this phenomenon using quantum mechanical transport theory and arrived at essentially the same results. In GQA the electrons (or holes), which have their velocity equal to the sound velocity, absorb phonons at specific values of the applied magnetic field for which these particular groups of electrons occupy energy states within  $kT$  of the Fermi energy. The resultant attenuation of the sound wave appears in the form of sharp peaks which are periodic in  $1/H_0$ . This period is usually very close to that of the de Haas-van Alphen oscillations.

The condition for observing well-defined  $\Delta n=0$  GQA peaks, first given by Gurevich *et al.*<sup>1)</sup> is

$$ql_F \left( \frac{\hbar\omega_c}{\varepsilon_F} \right)^{1/2} \gg 1, \quad (1)$$

where  $q$  is the wave vector of the sound wave;  $l_F$  is the mean free path of carriers at Fermi surface;  $\omega_c$  is the cyclotron frequency of carriers; and  $\varepsilon_F$  is the Fermi energy.

Such GQA was first observed experimentally in zinc by Korolyuk *et al.*<sup>3)</sup> Shapira *et al.*<sup>4)</sup> have made a detailed study of GQA in gallium.

\* Work supported in part by the U. S. Office of Naval Research and the Advanced Research Projects Agency.

A preliminary observation of this phenomenon in bismuth was reported by Korolyuk,<sup>5)</sup> Toxen *et al.*<sup>6)</sup> studied GQA in bismuth with  $H_0$  nearly perpendicular to the direction of the sound wave propagation. These earlier studies were, however, limited to fields under 17 kG. In the present work, we have carried out GQA experiments in bismuth for the Faraday configuration ( $H_0 \parallel q$ ), using fields up to 100 kG as a tool for studying the Fermi surface of electrons and holes.

### § 2. Experimental

The higher the frequency of the sound wave and the greater the mean free path of the carriers, the easier it is to satisfy the condition for observing GQA (eq. (1)). Thus most of the experiments were carried out at 930 Mc. The resistivity ratio  $\rho(300^\circ\text{K})/\rho(4.2^\circ\text{K})$  of the bismuth single crystal used in this experiment is about 500, and  $ql_F$  is estimated to be as high as 200 at 930 Mc. The condition for observing  $\Delta n=0$  GQA was therefore easily satisfied at a few kG for light carriers. To satisfy this condition for heavy carriers, the measurements were carried out at fields up to 100 kG. The experimental apparatus and sample preparation are described in the paper of magneto-acoustic geometric resonance in bismuth.<sup>7)</sup>

### § 3. Results and Discussions

Typical attenuation curves vs. magnetic field

are shown in Figs. 1, 2 and 3 for  $H_0$  and  $q$  along a binary, a bisectrix and the trigonal axes, respectively. From these data we are able to derive following information:

- A) accurate estimates of the cross-sectional areas of Fermi surface (from the periods)
- B) ratios of the spin masses to the cyclotron masses (from spin splittings)

C) some information of the energy band model (from the line shape)

D) motions of the Fermi level as a function of magnetic field (from the peaks at high field)

E) The existence of non-linear effect in the attenuation constant (from the relative height of the attenuation peaks)

These subjects will be discussed in the following sections.

A. Period

It is possible to determine  $1/H_0$  periods very accurately from the GQA attenuation curves,

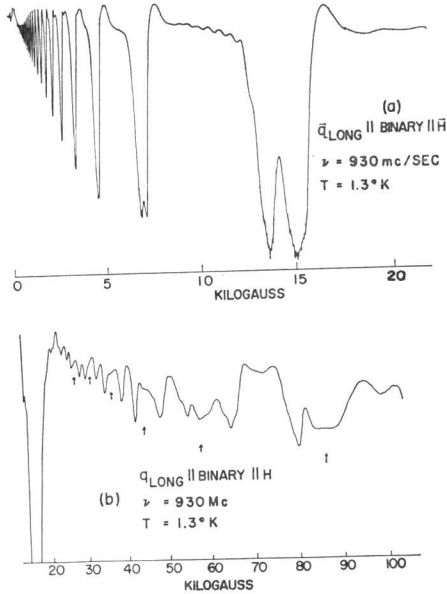


Fig. 1. Magnetic field dependence of the acoustic attenuation with magnetic field and sound wave propagation along a binary axis.

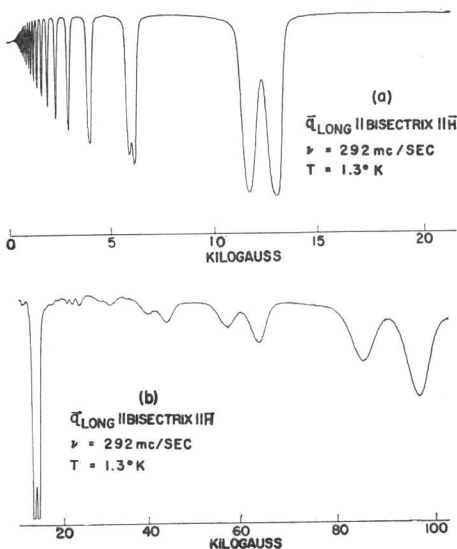


Fig. 2. Magnetic field dependence of the acoustic attenuation with magnetic field and sound wave propagation along a bisectrix axis.

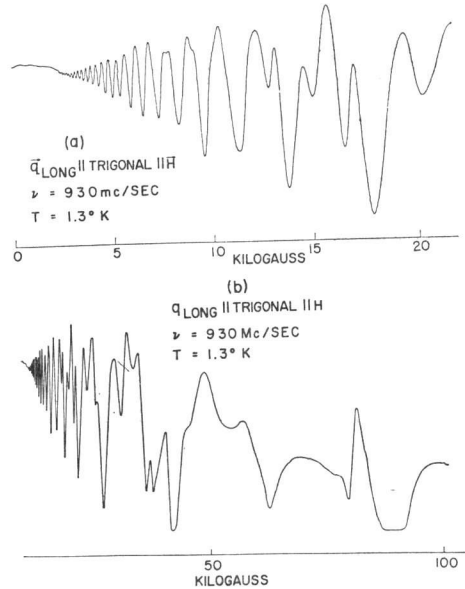


Fig. 3. Magnetic field dependence of the acoustic attenuation with magnetic field and sound wave propagation along the trigonal axis.

Table I. Periods of GQA compared with dHva periods obtained by previous workers.

$H_0$	Periods $\times 10^{-5}$ gauss $^{-1}$		Brandt <sup>(b)</sup>
	Present Work	Schoenberg <sup>(a)</sup>	
(Electrons)			
Binary	$0.53 \pm 0.05$ $7.15 \pm 0.01$	0.25 7.4	
Bisectrix	$8.45 \pm 0.05$	8.5 4.3	8.2 4.3
Trigonal	$1.2 \pm 0.2$	1.18	1.2
(Holes)			
Binary } Bisectrix }	$0.5 \pm 0.05$		0.41
Trigonal	$1.62 \pm 0.01$		1.6

a) D. Schoenberg: Phil. Trans A 245 (1952) 1.

b) See ref. 15).

because the attenuation peaks are spike shaped. The  $1/H_0$  plots of the peak positions vs. Landau number for the low field data exhibit accurate linear relations.

The main peaks for  $H_0$  along a binary and a bisectrix axes are due to electron ellipsoids (Figs. 1 (a) and 2(a)). They are found to have periods  $\Delta(1/H_0) = (7.15 \pm 0.01) \times 10^{-5} \text{ gauss}^{-1}$  and  $\Delta(1/H_0) = (8.45 \pm 0.05) \times 10^{-5} \text{ gauss}^{-1}$  respectively. The attenuation peaks corresponding to the hole ellipsoid were not observed in the low field region for these two configurations.

The main peaks appearing for  $H_0$  along the trigonal axis are due to the hole ellipsoid. (Fig. 3 (a)). The period for this series of attenuation peaks is  $\Delta(1/H_0) = (1.62 \pm 0.01) \times 10^{-5} \text{ gauss}^{-1}$ . A weak beat signal appears superposed on the main peaks in the low field region and becomes distinct above 10 kG. These were assigned to the electron peaks with spin splitting. From these assignments we obtain the value for the period  $\Delta(1/H_0) = (1.2 \pm 0.2) \times 10^{-5} \text{ gauss}^{-1}$  for the electron ellipsoids.

We believe that those values for the periods with the exception of the electron period for the trigonal axis are the most accurate values obtained so far. They are compared in Table I with the data of previous workers.

### B. Spin splittings

Spin splittings in bismuth have been observed in magnetothermal oscillations,<sup>8)</sup> the de Haas-van Alphen effect<sup>9)</sup> and Shubnikov-de Haas effect.<sup>10)</sup> If we include a "spin" term in the energy expression for the non-parabolic model,<sup>11)</sup> the magnetic field strength where GQA peaks appear is given by the following relations.

$$\begin{aligned} \varepsilon_F(1 + \varepsilon_F/\varepsilon_g) &= \hbar\omega_c(n + \varphi) + \frac{P_{z0}^2}{2m_z} \\ \varphi &= 1/2(1 \pm \Delta), \quad \Delta = m_c/m_s, \\ m_s &= 2m_0/g, \quad \left. \frac{\partial \varepsilon}{\partial P_z} \right|_{P_{z0}} = v_s \end{aligned} \quad (2)$$

where  $\varepsilon_g$  is the energy gap,  $v_s$  is the sound velocity,  $m_z$  is the longitudinal mass,  $m_c$  is the cyclotron mass and  $m_s$  is the spin mass of the carriers respectively. When the spin mass is fairly close to the cyclotron mass ( $\Delta \sim 1$ ) or when spin mass is fairly large compared with the cyclotron mass ( $\Delta \sim 0$ ), the attenuation peaks would exhibit splittings relatively small compared with the separation between the peaks (Fig. 1 (a) or Fig. 2 (a)). These two cases ( $\Delta \sim 1$  and  $\Delta \sim 0$ ), however, can be distinguished by

the phase  $\varphi$  of the series of the peaks, which can be obtained from the  $1/H_0$  plots of the peaks vs. Landau number. The values of  $\Delta$  obtained are 1.10, 1.11 and 0.7 for the electron ellipsoids for  $H_0$  along a binary, a bisectrix and the trigonal axes respectively. No spin splitting was observed for the hole attenuation peaks in the low field region.

The absolute values of spin masses and cyclotron masses can be calculated from  $1/H_0$  periods and the values of  $\Delta$ , providing the value for  $\varepsilon_F$  and  $\varepsilon_g$  are known. We will come back to this point later.

### C. Line shape

If one neglects the collisional broadening of Landau levels, the line shape depends only on the functional form of  $\varepsilon(H_0, P_z)$ . For a parabolic energy band model, the line shape is given by

$$\Gamma = \Gamma_0 \frac{\hbar\omega_c}{kT} \cosh^{-2} \left\{ \frac{\hbar\omega_c(n+1/2) - \varepsilon_F}{2kT} \right\}. \quad (3)$$

And the width  $\delta H$  of the peaks at half height is given by<sup>4)</sup>

$$\delta H/H = 3.53 kTP/\beta, \quad (4)$$

where  $P$  is the period of peaks and  $\beta = e\hbar/m_c c$ . However, if we assume a non-parabolic energy band model;

$$\begin{aligned} \varepsilon(1 + \varepsilon/\varepsilon_g) &= \hbar\omega_c(n + \varphi) + P_z^2/2m_z \\ \omega_c &= \frac{eH}{m_c(0)c}, \quad m_c(0) = \frac{m_c(\varepsilon_F)}{1 + 2\varepsilon_F/\varepsilon_g} \end{aligned} \quad (5)$$

(where  $m_c(0)$  and  $m_c(\varepsilon_F)$  are the cyclotron masses of carriers at the bottom of the band and at the Fermi surface respectively), the line shape becomes

$$\begin{aligned} \Gamma &= \Gamma_0 \frac{\hbar\omega_c}{kT} \cosh^{-2} \\ &\times \left[ \frac{\{(4\beta H/\varepsilon_g(n + \varphi) + 1)^{1/2} - 1\} \varepsilon_g/2 - \varepsilon_F}{2kT} \right]. \end{aligned} \quad (6)$$

And the width is given by

$$\delta H/H = 3.53 kT \sqrt{(P/\beta)^2 + (4/\varepsilon_g)(P/\beta)}, \quad (7)$$

where

$$\beta = e\hbar/m_c(0)c.$$

We calculate  $m_c(\varepsilon_F)$  from eqs. (4) and (7) for the electron peaks with  $H_0$  parallel to the bisectrix axis (Fig. 2 (a)). The  $\delta H_0/H_0$  is estimated to be approximately  $2.5 \times 10^{-2}$ . The value of  $m_c$  obtained from eq.(4) is  $m_c(\varepsilon_F)/m_0 = 0.009$ . On the other hand, eq. (7) yields a value  $m_c(\varepsilon_F)/m_0 =$

0.010. We have assumed here  $\epsilon_F = 27.6 \text{ meV}^{(10)}$  and  $\epsilon_g = 15.3 \text{ meV}^{(12)}$ . The value for  $m_c/m_0$  obtained directly from cyclotron resonance experiments<sup>13,14)</sup> is 0.009. We can not yet draw any definite conclusion from this evaluation about which model should be taken for bismuth, because this estimate of  $\delta H_0/H_0$  can include a rather large error. However, a more careful analysis of the line shape may provide us with a powerful tool for studying the energy band model.

#### D. Analysis of high field data

Figures 1 (b), 2 (b) and 3 (b) are the typical high field data of the attenuation vs. magnetic field with  $H_0$  and  $q$  parallel to a binary, a bisectrix and the trigonal axes respectively. The attenuation peaks corresponding to the hole ellipsoid and the electron ellipsoids which have large cyclotron masses are the main points of interest in this region.

The main attenuation peaks for  $H_0$  and  $q$  parallel to a binary axis and a bisectrix axis (Fig. 1(b), Fig. 2(b)) correspond to the hole ellipsoid and exhibit paring due to spin splitting. These peaks are found to have a period of  $0.5 \times 10^{-5} \text{ gauss}^{-1}$  for both directions, which is larger than the value  $0.41 \times 10^{-5} \text{ gauss}^{-1}$  obtained by Brandt<sup>15)</sup> from low field de Haas-van Alphen experiments. This discrepancy can be explained by the gradual decrease of the Fermi level with increasing field in these directions, which was observed by Smith *et al.*<sup>10)</sup> The weak peaks, marked by arrows in Fig. 1 (b) are attributed to the electron ellipsoid whose major axis is in the binary plane. This period is estimated to be  $0.53 \times 10^{-5} \text{ gauss}^{-1}$  which agrees with that of the weak oscillations appearing in 10 kG region for the same configuration.

For  $H_0$  and  $q$  parallel to the trigonal axis the positions and shapes of the attenuation peaks are very complicated (Fig. 3 (b)). (The flattening of the attenuation peaks at 40 kG and at 90 kG is due to the logarithmic scale of the attenuation measurements and manifests itself when the attenuation exceeds 20 db.) The complication is mainly due to the fact that the period of the electron ellipsoids is close to that of the hole ellipsoid. The spin splitting of the electron attenuation peaks provides an additional complication.

The main peaks were observed at 25 kG, 41 kG and at 90 kG (Fig. 3 (b)). However, the extrapolation of low field data for  $H_0$  parallel to the trigonal axis predicts peak positions at

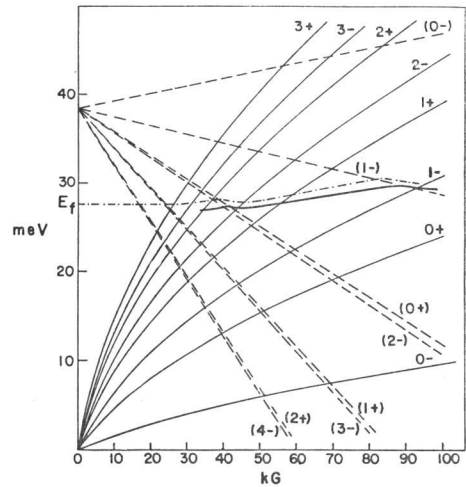


Fig. 4. Magnetic field dependence of the electron Landau levels and hole Landau levels. Solid lines represent electron levels and broken lines represent hole levels. Numerical values are taken from the data of Smith *et al.*<sup>10)</sup>

25 kG, 42 kG and 130 kG. This indicates an increase of the Fermi level with increasing magnetic field. The other minor peaks are attributed tentatively to the spin split electron peaks. To understand the positions of electron attenuation peaks we plot in Fig. 4 the Landau levels of electrons and holes as a function of magnetic field using the mass parameters of Smith *et al.*<sup>10)</sup>. Electron Landau levels are not linear because of non-parabolicity of the bands. If we use the magnetic field dependence of the Fermi level from Smith *et al.*<sup>10)</sup> the hole peaks are expected to appear at 40 kG and at 82 kG which do not agree with the present data. However, if we assume that the Fermi energy at zero field is 26.6 meV which is 1 meV lower than the values used by Smith *et al.*, the expected values of the field strength for the hole peaks coincide with experimentally observed values. Similarly the electron attenuation peaks for  $H_0$  along the trigonal axis are predicted at 34, 44, 56 and 92 kG. The peaks were experimentally observed at 35, 44, 63 and 80 kG. Thus the analysis is not yet perfect for this configuration. The energy level of electrons for the field along trigonal axis is still open to future study.

It is of interest to note in Fig. 4 that the electron (2-) level and the hole (2-) level cross the Fermi level almost simultaneously at 90 kG. Although these coincidences are accidental, they may partially account for the extremely large

Table II. Cyclotron masses and spin masses.

$H_0$	mass	electron		hole
Binary	$m_e$	.0101(.0097)*	.131(.128)	.19 (.21)
	$m_s$	.0092(.0091)	—(.36)	.5 (1.5)
Bisectrix	$m_e$	.0086(.0084)	.017(.0168)	.19 (.21)
	$m_s$	.0077(.0079)	.016(.0158)	.5 (1.5)
Trigonal	$m_e$	.060 (.065)		.061(.064)
	$m_s$	.10 (.11)		—(.033)

\* The values in the parenthesis are taken from ref. 10).

attenuations at 40 kG and 90 kG with  $H_0$  along the trigonal axis.

Finally, values for cyclotron masses and spin masses were calculated from the periods of the peaks and the spin splittings assuming 26.6 meV for the value of the Fermi energy and 15.3 meV for the energy gap.<sup>12)</sup> These values are compared with the data of Smith *et al.*<sup>10)</sup> in Table II. The agreements are reasonably good except for the spin masses of the hole for  $H_0$  along a binary and a bisectrix axes. The large discrepancy of these spin masses may perhaps be explained by a misorientation of the crystal of about 0.5 degree.

#### E. Non-linear effects

For  $H_0$  and  $q$  along a bisectrix axis, only one set of attenuation peaks is observed corresponding to the ellipsoid whose longest axis is in the bisectrix-trigonal plane. The absence of the attenuation peaks for the two other equivalent electron ellipsoids is attributed to a non-linearity of the attenuation caused by the building up of a transverse magneto-acousto electric field.<sup>16)</sup> This TMA electric field is set up by the lateral translation of the centers of the orbits of the electrons in ellipsoids whose axes are tilted from the direction of the applied magnetic field. The TMA electric field, which has not been taken into account in the usual theory of giant quantum attenuation, causes tilting of the Fermi level and, thereby, a decrease in the ratio of phonon absorption to the phonon emission.<sup>17)</sup> The TMA field and the corresponding acoustic attenuation constant are respectively given by

$$E = \frac{E_0}{1 + 1/\beta}, \quad \Gamma = \frac{\Gamma_0}{1 + \beta},$$

where  $E_0$  is the critical field for the sound wave amplification,  $\Gamma_0$  is the attenuation constant in the absence of the TMA field. The non-linear constant  $\beta$  is given by

$$\beta = \frac{4\pi N}{kT} \left( \frac{c\hbar q}{H_0} \right)^2 \gamma \tau f(\alpha),$$

where  $N$  is the phonon flux,  $q$  is the phonon wave number,  $\gamma$  is the phonon absorption rate constant,  $\tau$  is the decay time-constant of the TMA field and  $f(\alpha)$  is a function of mass anisotropy. Under the conditions of our experiment  $\beta$  is estimated to be greater than unity so that  $E_{\text{TMA}} \approx E_0$ . Direct measurements of the  $E_{\text{TMA}}$  are now being carried out for various configurations of  $q$  and  $H_0$ .

#### Acknowledgements

The authors wish to thank Dr. J. E. Kunzler for supplying us a pure crystal of bismuth used in this experiment. Technical assistance of Mr. V. G. Chirba and Mr. H. W. Dail are also acknowledged.

#### References

- 1) V. L. Gurevich, V. G. Skobov and Yu A. Firsov: Soviet Physics-JETP **13** (1961) 552.
- 2) J. J. Quinn: Phys. Rev. **137** (1965) A 889.
- 3) A. P. Korolyuk and T. A. Prushak: Soviet Physics-JETP **14** (1962) 1201.
- 4) Y. Shapira and B. Lax: Phys. Rev. **138** (1965) A 1191.
- 5) A. D. Korolyuk: Soviet Physics-Solid State **5** (1964) 2433.
- 6) A. M. Toxen and S. Tansel: Phys. Rev. **137** (1965) A 211.
- 7) Y. Sawada and E. Burstein: to be published.
- 8) J. E. Kunzler, F. S. L. Han and W. S. Boyle: Phys. Rev. **128** (1962) 1084.
- 9) Y. Saito: J. Phys. Soc. Japan **18** (1963) 1845.
- 10) G. E. Smith, G. A. Baraff and J. M. Rowell: Phys. Rev. **135** (1964) A 1118.
- 11) B. Lax, J. G. Mavroides, H. J. Zeiger and R. J. Keyes: Phys. Rev. Letters **5** (1960) 241.
- 12) R. N. Brown, J. G. Mavroides and B. Lax: Phys. Rev. **129** (1963) 2055.
- 13) G. E. Smith, L. C. Hebel and S. J. Buchsbaum: Phys. Rev. **129** (1963) 154.

- 14) Yi-Han Kao: *Phys. Rev.* **129** (1963) 1122.
- 15) N. B. Brandt: *Zh. eksper. teor. Fiz.* **38** (1960) 1355; N. B. Brandt and M. V. Razumenko: *Zh. eksper. teor. Fiz.* **39** (1960) 276.
- 16) Y. Sawada, E. Burstein and L. Testardi: to be published.
- 17) R. F. Kazarinov and V. G. Skobov: *Soviet Physics-JETP* **16** (1963) 1057.